IEEE Access
Multidisciplinary ⋮ Rapid Review ⋮ Open Access Journal

Received 6 February 2024, accepted 21 April 2024, date of publication 6 May 2024, date of current version 17 May 2024.

Digital Object Identifier 10.1109/ACCESS.2024.3397571

RESEARCH ARTICLE

Development of an Electrochemical Dopamine Sensor Using Nitrogen-Rich Sulfur Dual-Doped Reduced Graphene Oxide

J. LAVANYA[1,2], M. AAKASH[2], A. RAVI SANKAR[1,3], (Senior Member, IEEE), AND N. GOMATHI[4]

[1]Center for Innovation and Product Development (CIPD), Vellore Institute of Technology (VIT), Chennai Campus, Chennai, Tamil Nadu 600127, India
[2]Division of Physics, School of Advanced Sciences (SAS), Vellore Institute of Technology (VIT), Chennai Campus, Chennai, Tamil Nadu 600127, India
[3]School of Electronics Engineering (SENSE), Vellore Institute of Technology (VIT), Chennai Campus, Chennai, Tamil Nadu 600127, India
[4]Department of Chemistry, Indian Institute of Space and Technology, Thiruvananthapuram, Kerala 695547, India

Corresponding author: A. Ravi Sankar (ravisankar.a@vit.ac.in)

The experimental research work, open-access publication, post-doctoral fellowship (awarded to the author J. Lavanya), and doctoral research fellowship (awarded to the author M. Aakash) were supported by the VIT, Chennai Campus.

ABSTRACT In the present work, we report on developing an electrochemical dopamine sensor using a novel material of nitrogen-rich sulfur dual-doped reduced graphene oxide (N-rich SRGO). Nitrogen and sulfur heteroatoms were incorporated into graphene sheets through a one-step, cost-effective hydrothermal approach to synthesize N-rich SRGO. Experimental investigations were carried out to compare the electrochemical properties of N-rich SRGO with nitrogen sulfur-doped reduced graphene oxide (NSRGO), nitrogen-doped reduced graphene oxide sheets (NRGO), and reduced graphene oxide (RGO) by modifying the glassy carbon electrode. Electrochemical studies demonstrated that N-rich SRGO exhibited a notably higher oxidation current (345 μA) compared to NSRGO (219 μA), NRGO (173 μA), and RGO (160 μA). We developed a dopamine sensor by utilizing the superior chemical reactivity and enhanced charge carrier density of the proposed N-rich SRGO-modified electrode. Experimental results reveal a high sensitivity of 142 μA/mM, with a limit of detection of 9.3 μM and a wide dynamic range of 150-350 μM. This N-rich SRGO-based sensor displayed excellent repeatability and selectivity, even in the presence of other electroactive interferents, showcasing its potential for practical applications.

INDEX TERMS Dopamine, differential pulse voltammetry, electrochemical sensor, hydrothermal process, nitrogen-rich sulfur dual-doped reduced graphene oxide.

I. INTRODUCTION

The effectiveness of electrochemical sensors hinges on critical factors such as rapid electron transfer rate, ample surface area, prompt response, high electrical conductivity, and a broad potential window of the working electrode [1]. Diverse strategies have been explored to enhance electrochemical sensor performance by modifying the working electrode with various materials [2]. Notably, graphene has emerged as a preferred material for electrochemical sensing due to its superior attributes, including enhanced electron transfer kinetics [3], substantial surface area of 2630 m^2/g [4], excellent electrical conductivity [5], and an extensive potential window [6]. Despite graphene's excellent electrochemical properties, its uniform charge distribution and restacking property hinder the active sites and reduce the interaction between the analytes and graphene material [7], [8], [9]. Extensive research endeavors have focused on tailoring graphene's physical and chemical attributes through structural and chemical modifications to optimize electrocatalytic properties [10], [11]. Significantly, a prevalent approach to enhancing the chemical and electrical properties involves

The associate editor coordinating the review of this manuscript and approving it for publication was Lei Wang.

chemical modification with heteroatoms such as nitrogen, boron, sulfur, and phosphorous. These dopant atoms play a pivotal role in dislocating the sp^2 structure and fine-tuning the band structure, resulting in alterations to spin density, Fermi level, and the localized electronic state of graphene [12], [13], [14].

Moreover, introducing chemical moieties through heteroatom doping on the graphene structure improves the electron transfer rate between the sensing material and electrolyte and serves as anchoring sites for analytes. For instance, nitrogen (N)-doped graphene has found widespread use in sensing various analytes, including nitrite, nicotine, acetaminophen, and simultaneous detection of ascorbic acid (AA), dopamine (DA), uric acid (UA), [15], [16], [17], [18]. Similarly, sulfur (S)-doped graphene has been synthesized and applied for the electrochemical detection of gallic acid, DA, and hydrogen peroxide [19], [20], [21].

In addition, research has demonstrated that the electrocatalytic properties of graphene can be substantially improved by incorporating dual heteroatoms, specifically N and S, as opposed to mono-atom doping [22], [23]. In recent years, a few studies have addressed the electrochemical sensing of diverse analytes using nitrogen-sulfur co-doped reduced graphene oxide (NSRGO). For example, Zhang et al. developed a nitrogen-sulfur co-doped graphene nanoribbon sensor for detecting 2, 4, 6-trinitrotoluene [24]. Additionally, Tian et al. utilized NSRGO in both non-enzymatic [25] and enzymatic [26] approaches to sense glucose. Guo et al. successfully detected Pb^{2+} and Cd^{2+} simultaneously with higher sensitivity and selectivity than mono-heteroatom-doped RGO using NSRGO [27]. Another research group synthesized nitrogen-sulfur-activated RGO to detect catechol and hydroquinone simultaneously [28]. Recently, Han et al. investigated the sensing capabilities of nitrogen-sulfur dual-doped RGO for fenitrothion detection [29]. Despite the superior electrocatalytic activity of NSRGO compared to mono-heteroatom-doped RGO, the pyridinic N group has been identified as a significant contributor to the enhanced electrocatalytic property of graphene [30]. However, there is a notable gap in the existing research literature regarding the augmentation of nitrogen content to achieve nitrogen-rich sulfur dual-doped reduced graphene oxide (N-rich SRGO) for electrochemical sensing. Consequently, the present study addresses this gap by synthesizing N-rich SRGO through a cost-effective and non-toxic hydrothermal approach. The synthesized material is then applied to quantify the concentration of DA accurately.

Dopamine, chemically known as 3,4-dihydroxyphenylethylamine, serves as a monoamine neurotransmitter released by neurons in anticipation of pleasure within the human or animal brain. This neurotransmitter is pivotal in various bodily functions, including memory, attention, heart rate, and kidney function. In healthy human body fluids, dopamine levels typically range from 0 to 0.25 nM in blood and 0.3 to 3 μM in urine. Aberrations in dopamine levels, either low or high, are correlated with a multitude of maladies, including Alzheimer's, Parkinson's, cancer, and HIV infection [31]. Precise and cost-effective sensors for dopamine detection are essential due to their critical role in health. Several analytical techniques are available for quantifying dopamine levels, including optical fiber-based sensors [32], spectrometry [33], chemiluminescence [34], fluorescence [35], and plasmonic-based sensors [36]. Despite the high sensitivity of these techniques, drawbacks such as time-consuming processes, tedious sample preparation protocols, high costs, and the requirement for trained personnel limit their utility in achieving rapid, sensitive, and effective dopamine detection. In contrast, the electrochemical sensing technique proves suitable for cost-effective, rapid, easy, compact, and in-situ detection [37], [38], [39], [40], [41].

This research article introduces the synthesis and utilization of N-rich SRGO in an electrochemical DA sensor. The manuscript is structured as follows: In Section I, essential characteristics that improve the performance of electrochemical sensors are examined, including the characteristics of graphene and the utilization of heteroatoms doped graphene in electrochemical sensing. It also includes a concise overview of dopamine and its electrochemical sensing methods. Section II provides insights into the synthesis and preparation of N-rich SRGO-modified electrodes. Section III offers a comprehensive discussion on the material and electrochemical characterization of N-rich SRGO, exploring its application in electrochemical dopamine sensing. Lastly, Section IV presents the concluding remarks on the role of N-rich SRGO in advancing the electrochemical sensing of dopamine.

II. EXPERIMENTAL DETAILS

A. REAGENTS

Graphite synthetic, potassium ferricyanide, potassium ferrocyanide, 99% thiourea, extra pure urea, potassium chloride, potassium phosphate monobasic, acetone, sodium phosphate dibasic dopamine, ascorbic acid, uric acid, sodium chloride, and ethanol were received from Sisco Research Laboratories Pvt. Ltd. India. 88% ACS ortho phosphoric 98% sulfuric acid, 30% hydrogen peroxide, potassium permanganate, 35% hydrochloric acid, 80% hydrazine hydrate, N, N-Dimethylformamide (DMF) were procured from Merck, India. Without additional purification, all chemicals purchased in the analytical grade were used. Millipore water (18.2 MΩ) was used to prepare each stock solution.

B. SYNTHESIS OF NITROGEN-RICH SULFUR DUAL-DOPED REDUCED GRAPHENE OXIDE

The improved Hummers method was employed to exfoliate graphite to obtain graphene oxide (GO) [42]. GO, thiourea, and urea were taken in the ratio of 1:2:4 and dispersed (1mg/ml) in distilled water to synthesize N-rich SRGO, as illustrated in Fig.1. The mixture was transferred from a sonicator to a Teflon beaker and autoclaved at 120 °C for 12 h. The obtained product was subsequently washed with

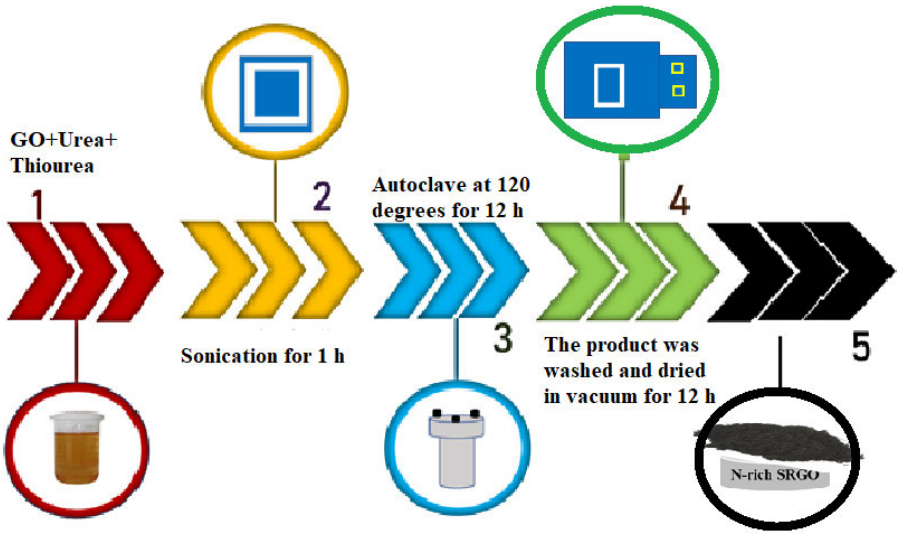

FIGURE 1. A pictorial representation of the hydrothermal synthesis of N-rich SRGO.

acetone and distilled water before being dried overnight at 60 °C in a vacuum oven. We also synthesized RGO, NRGO, and NSRGO materials and compared their electrocatalytic activity with N-rich SRGO. In brief, the RGO was prepared hydrothermally using GO dispersion at 120°C for 12 h. NSRGO and NRGO were synthesized through a similar process using thiourea or urea alone, respectively.

C. MATERIAL CHARACTERIZATION TECHNIQUES

The crystalline structure of the heteroatom-doped RGO was examined using X-ray diffraction (XRD) (Rigaku with CuKα radiations λ =1.5406 Å). The chemical composition of heteroatom-doped RGO was investigated from the Raman spectra acquired between 500 and 3000 cm^{-1} using a Renishaw spectrometer and a 532 nm laser. Using a Field Emission Scanning Electron Microscope (FE-SEM) and energy-dispersive X-ray spectroscopy (EDS) (FEI QUANTA 250 FEG), the chemical structure and the surface morphology of the obtained materials were analyzed.

D. ELECTROCHEMICAL MEASUREMENTS

All electrochemical measurements, including electrochemical impedance spectroscopy (EIS), cyclic voltammetry (CV), amperometric measurements, and differential pulse voltammetry (DPV), were carried out at ambient temperature using the Squidstat^{TM} plus potentiostat (Admiral, France). The electrochemical studies were performed on a 3 mm diameter glassy carbon electrode (GCE) as the working electrode, a silver/silver chloride (Ag/AgCl) electrode as the reference electrode, and a platinum (Pt) wire as the counter electrode. DA sensing experiments were conducted in a phosphate buffer solution (PBS).

E. PREPARATION OF MODIFIED ELECTRODE

Using 0.05 mm alumina particles, the GCE was polished, rinsed in millipore water and ethanol for 2-3 min, and dried under an inert atmosphere. Following modification with 7 μl of N-rich SRGO suspension *via* drop casting, the polished GCE was desiccated under vacuum at room temperature for 8 h. For better dispersion, the synthesized heteroatom-doped RGO materials were dispersed in DMF (1 mg/1 ml) via ultrasonication for 30 minutes.

III. RESULTS AND DISCUSSION

A. CRYSTALLINITY AND PURITY OF THE MATERIALS

The increase in interlayer spacing with a slight blue shift in the graphitic peak observed in Fig.2 (a) of NRGO (24.5°, 3.61 Å), NSRGO (24.1°, 3.66 Å), and N-rich SRGO (23.8°, 3.75 Å), confirms the incorporation of heteroatoms into the carbon skeleton. Using Raman spectroscopy, the defect density and purity of reduced graphene oxide (RGO) doped with heteroatoms were determined; the results are depicted in Figure 2 (b). The 'G' band at 1580 cm^{-1} corresponds to the E_{2g} bond stretching of ordered graphitic carbon, whereas the 'D' band at 1350 cm^{-1} corresponds to the structural defects in the carbon skeleton. The D-band and G-band intensity ratio reveals graphitic and defect levels of carbon materials. Hence, the increase in $D_{intensity}/G_{intensity}$ ratios of NRGO (1.03), NSRGO (1.18), and N-rich SRGO (1.23) confirms the incorporation of nitrogen and sulfur-heteroatoms in carbon lattice [43].

B. SURFACE MORPHOLOGY AND ELEMENTAL COMPOSITION

The micrographs of heteroatom-doped RGO observed in FESEM images (Fig. 3(a-c)) infer no significant structural change in the crumpled sheet morphology. Furthermore, the considerable difference in the carbon, nitrogen, and sulfur concentrations of NRGO, NSRGO, and N-rich SRGO observed in EDS spectra (Fig.3(d-e)) confirms the effective doping of heteroatom in the graphitic skeleton. The

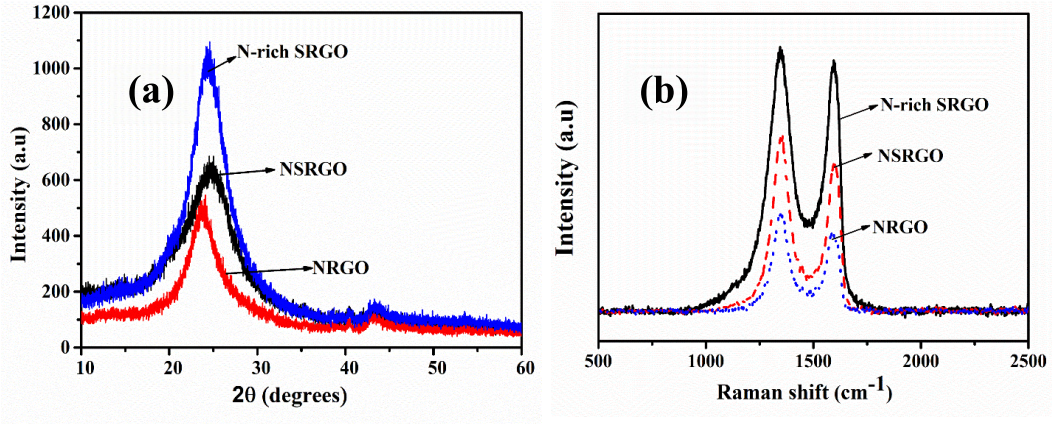

FIGURE 2. (a) X-ray diffraction and (b) Raman spectrum of NRGO, NSRGO, and N-rich SRGO.

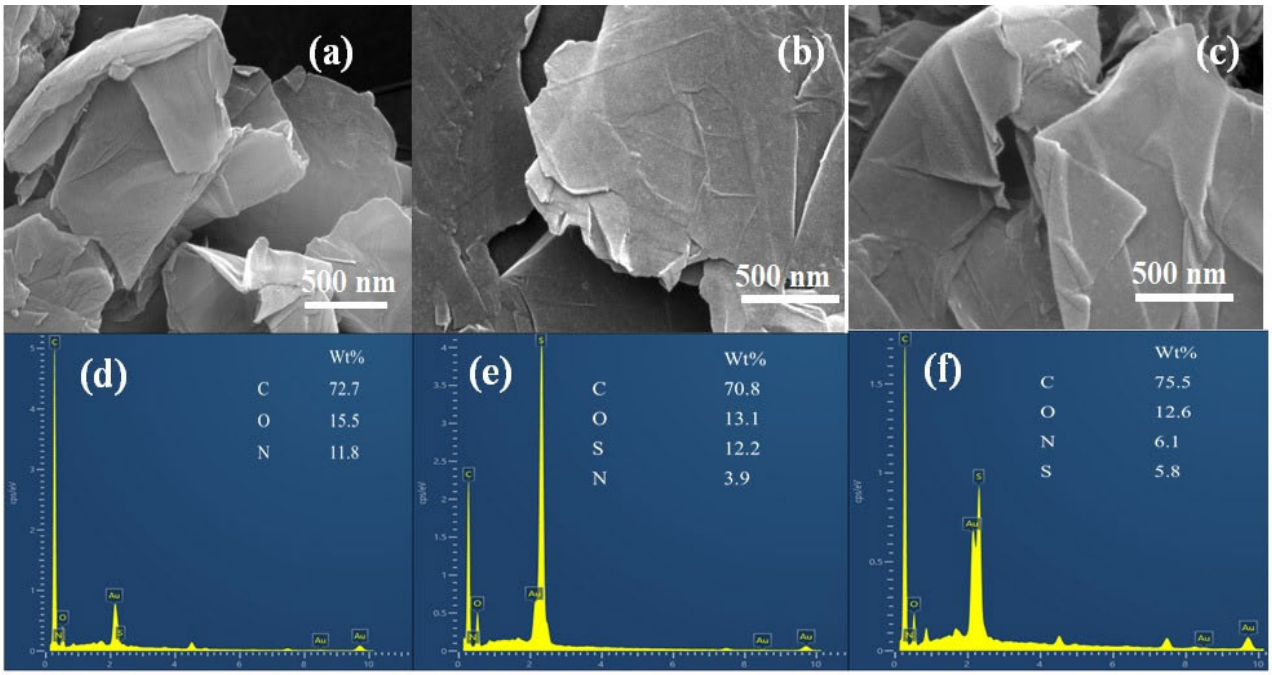

FIGURE 3. FESEM images of (a) NRGO, (b) NSRGO (c) N-rich SRGO and EDS of (d) NRGO, (e) NSRGO and (f) N-rich SRGO.

increase in the N content (Fig.3(e)) indicates the incorporation of more nitrogen atoms into the graphene structure.

C. ELECTROCHEMICAL BEHAVIOUR OF N-RICH SRGO TOWARDS POTASSIUM FERRO/FERRICYANIDE

The electrocatalytic properties of the modified electrodes were assessed through CV using the standard redox probe ferro/ferricyanide. The obtained CV results, as depicted in Fig. 4(a), showcase a higher peak current for the N-rich SRGO-modified electrode (345 μA) compared to NSRGO (219 μA), NRGO (173 μA), RGO (160 μA), and the bare glassy carbon electrode (GCE) (72 μA). This observation indicates that N-rich SRGO exhibits superior electrical conductivity and more active sites than RGO, NRGO, and NSRGO. Thus, N-rich SRGO with abundant electroactive sites accelerates the charge transfer between the analyte and electrode due to enhanced charge carrier density and high chemical activity offered by N and S heteroatoms.

We have conducted CV at various scan rates (10-100 mV/s) in 4 mM ferricyanide/0.1 M KCl (Fig.4b) to determine the electrochemical surface area (A_{ECSA}) of N-rich SRGO-modified electrode using the Randles–Sevcik equation (1) [44],

$$I_{pa} = 2.69 * 10^5 A_{ECSA} D^{1/2} n^{3/2} v^{1/2} C \quad (1)$$

where n is the number of electrons transferred, C indicates the bulk concentration of the analyte in mol/cm^3, and

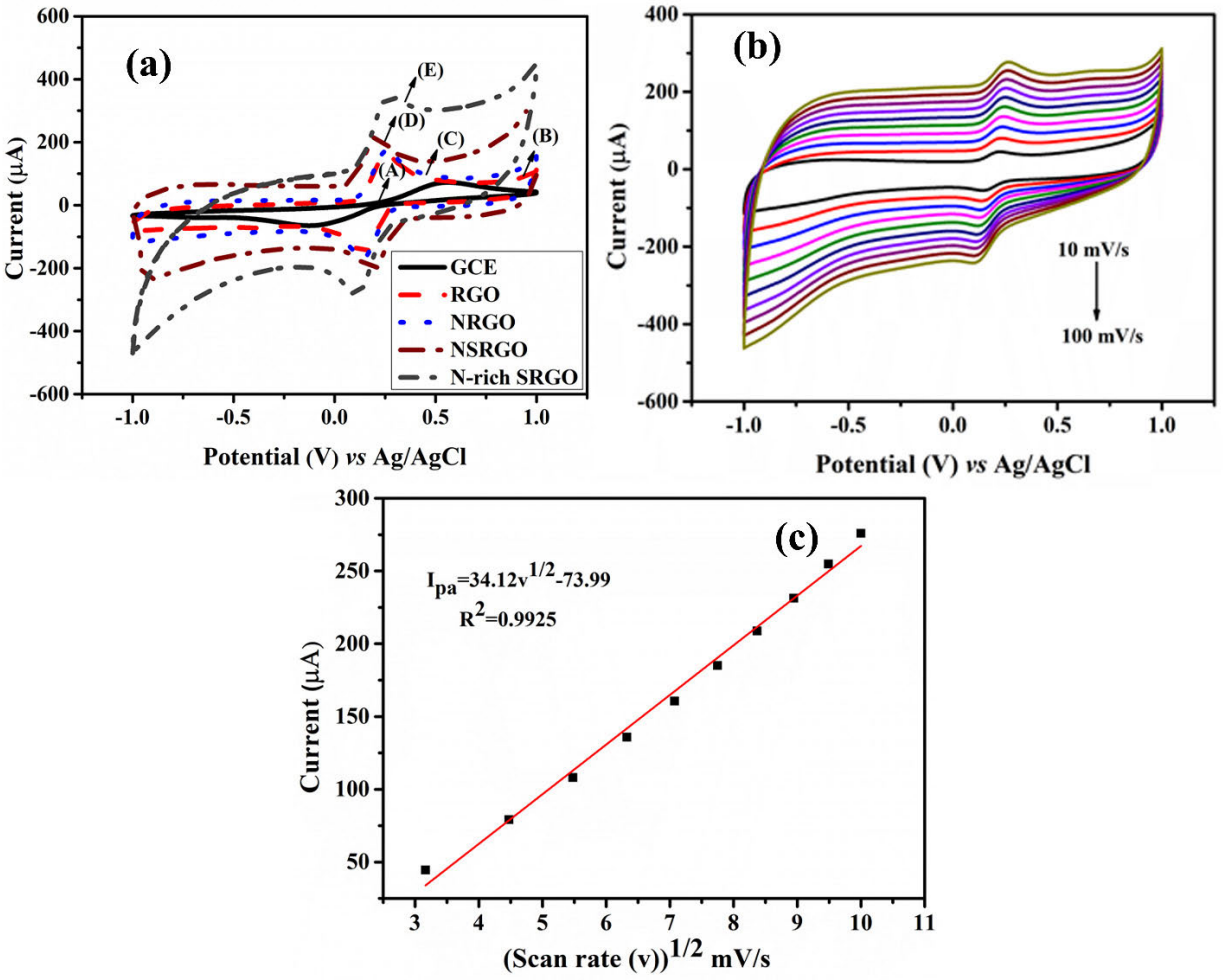

FIGURE 4. (a) Electrocatalytic activity of GCE and modified GCE was carried out in 5 mM Fe $(CN)_6^{3-/4-}$ in 0.1 M KCl (b) Electrochemical surface area (ECSA) of N-rich SRGO was determined by recording CVs at different scan rate (10-100mV/s) in 4mM ferricyanide in 0.1M KCl, (c) I_{pa} vs $(v)^{1/2}$.

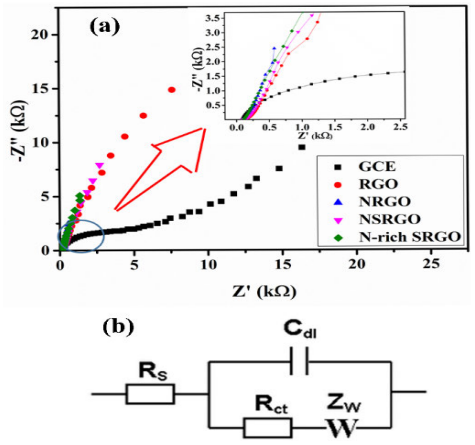

FIGURE 5. (a) The electrical conductivity of all modified electrodes was investigated in 5mM $Fe(CN)_6^{3/4}$ in 0.1 M KCl, (b) equivalent randles circuit.

D represents the diffusion constant of the analyte in cm^2/s. Using the slope value obtained from the plot I_{pa} vs. $v^{1/2}$ (Fig. 4c) in equation (1), the A_{ECSA} was estimated as 0.012 cm^2. The charge transfer resistance of the modified electrodes was determined through EIS in 5 mM $Fe(CN)_6^{3-/4-}$/0.1 M KCl, employing a constant AC potential of 10 mV/s within the frequency range of 10 mHz to 100 kHz. A semicircle in the higher frequency region of the Nyquist diagram (Fig. 5a) represents the charge transfer resistance (R_{ct}) of the modified electrodes. In contrast, an inclined line at lower frequencies indicates a diffusion-controlled process. By fitting the Nyquist plot using the Randle equivalent circuit (Fig. 5b), the calculated R_{ct} values were as follows: N-rich SRGO (4.89 mΩ), NSRGO (402 mΩ), NRGO (1.03 Ω), RGO (66.1 Ω), and GCE (1.22 kΩ). Consistent with the CV results, the reduced Rct value of the N-rich SRGO-modified electrode can be attributed to its excellent electrical conductivity, highlighting its commendable electrocatalytic activity.

D. ELECTROCHEMICAL SENSING OF N-RICH SRGO TOWARDS DOPAMINE

1) OPTIMIZATION OF pH

The sensor's performance relies on the electrochemical properties of the working electrode and the electrolyte's pH.

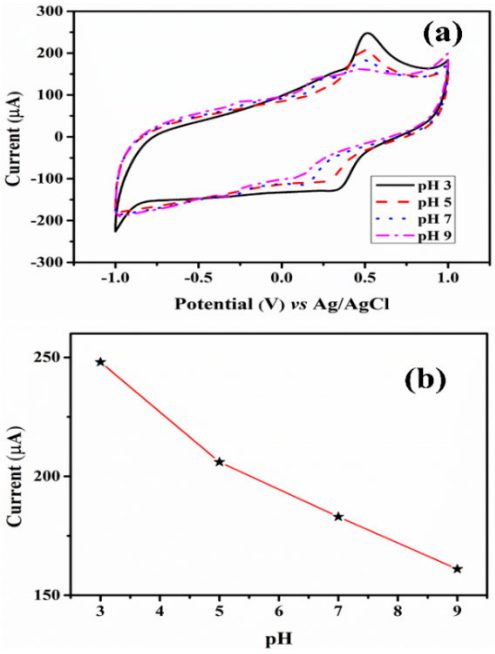

FIGURE 6. (a) pH studies from 3 to 9 in 0.1 M PBS, (b) plot of redox peak current vs pH.

Accordingly, we investigated the impact of electrolyte pH ranging from 3 to 9. As evident in Fig. 6 (a and b), an increase in pH corresponds to a decrease in the oxidation peak current. Notably, at pH 3, a higher DA oxidation current, marked by a distinct peak potential, was observed, indicating the necessity of proton involvement for optimal performance of the N-rich SRGO-modified electrode. Therefore, pH 3 was selected for further dopamine sensing. Also, the ratio of redox peak currents (I_{pa}/I_{pc}) was 1.97, which is characteristic of a quasi-reversible process for N-rich SRGO-modified electrodes.

2) ELECTRODE KINETICS

The kinetics of the N-rich SRGO-modified electrode towards 1 mM DA detection in 0.1 M PBS (pH 3.0) was examined by recording CVs at different scan rates. The relationship between the redox peak current and the scan rate (from 10 to 100 mV/s) is illustrated in Fig.7a. With a correlation coefficient of 0.998, the relationship between the square root of the scan rate and the redox peak current is linear, indicating that the electrochemical sensing reaction of N-rich SRGO towards DA is governed by a diffusion process. The surface coverage area of the N-rich SRGO was calculated using the equation (2),

$$I_{pa} = \frac{n^2F^2vA_{ECSA}\Gamma}{4RT} \tag{2}$$

where Γ represents the surface coverage, n is the number of transferred electrons, A_{ECSA} denotes the electrode's surface area in cm^2, F implies Faraday's constant, v represents scan rate in mV/s, R is the gas constant in J/K/Mol, T represents temperature in K. By substituting the slope value obtained from the plot I_{pa} vs v (Fig 7b) in equation (2), the surface coverage value of DA on the N-rich SRGO-modified electrode was calculated as $2.232^{*}10^{-5}$mol/cm^2 [45]. The diffusion coefficient (D) at the N-rich SRGO-modified electrode was calculated using equation (3) [46],

$$I_{pa} = 0.4463nFCA_{ECSA}v^{1/2}D^{1/2}(nF/RT)^{1/2} \tag{3}$$

Using the slope value from the plot $I_{pa}vs\ v^{1/2}$ in Fig 7(c), the D value was calculated as $2.3^{*}\ 10^{-11}$cm^2/s. The slope value (0.69) obtained from the plot (log I_p) vs. (log v) in Fig.7(d) confirmed that the electrode process is diffusion-controlled. The positive and negative shifts observed in oxidation and reduction potential in Fig.7(e) also confirm that the electrochemical oxidation of DA towards N-rich SRGO-modified electrode is a diffusion-controlled reaction. By using the slope value obtained from Fig.7(e), the electron-transfer coefficient (α) was determined using the equations (4) and (5) [47],

$$E_{pc} = E^{\circ'} - \left(\frac{RT}{\alpha nF}\right) lnv \tag{4}$$

$$E_{pa} = E^{\circ'} - \left(\frac{RT}{(1-\alpha)\,nF}\right) lnv \tag{5}$$

where α represents the electron-transfer coefficient, $E^{\circ'}$ denotes the formal potential in V, E_{pc} indicates the cathodic peak potential in V, and E_{pa} is the anodic peak potential in V. The calculated electron-transfer coefficient of 0.4 matches the theoretical value between 0.3 and 0.7 for diffusion-controlled processes [48].

3) DOPAMINE CONCENTRATION STUDIES

Under optimized conditions, we conducted DPV studies to assess the sensitivity, limit of detection (LOD), and limit of quantification (LOQ) of the developed sensor, as illustrated in Fig. 8. In Fig. 8a, an increase in peak current corresponding to the concentration of DA from 0 to 350 μM is evident within the potential window of 0.3 to 0.7 V, utilizing 0.1 M PBS at pH 3. The sensitivity of the N-rich SRGO-modified electrode was determined as 142 μA/mM from the slope of the calibration plot (Fig. 8b). The LOD and the LOQ were calculated using the equation [49] (6) and (7),

$$LOD = \frac{3\sigma}{Sensitivity} \tag{6}$$

$$LOQ = \frac{10\sigma}{Sensitivity} \tag{7}$$

where σ denotes the standard deviation of the blank voltammogram in μA, and *sensitivity* is the slope value obtained from the calibration plot in μA mM^{-1}. The LOD and LOQ were found to be 9.3 and 31 μM. A comparative analysis of the electrochemical sensing performance, encompassing LOD and sensitivity, of dopamine sensors using N-rich SRGO-modified electrodes is presented in Table 1 alongside findings from prior studies. Notably, the N-rich SRGO-modified electrode exhibited superior sensitivity, potentially

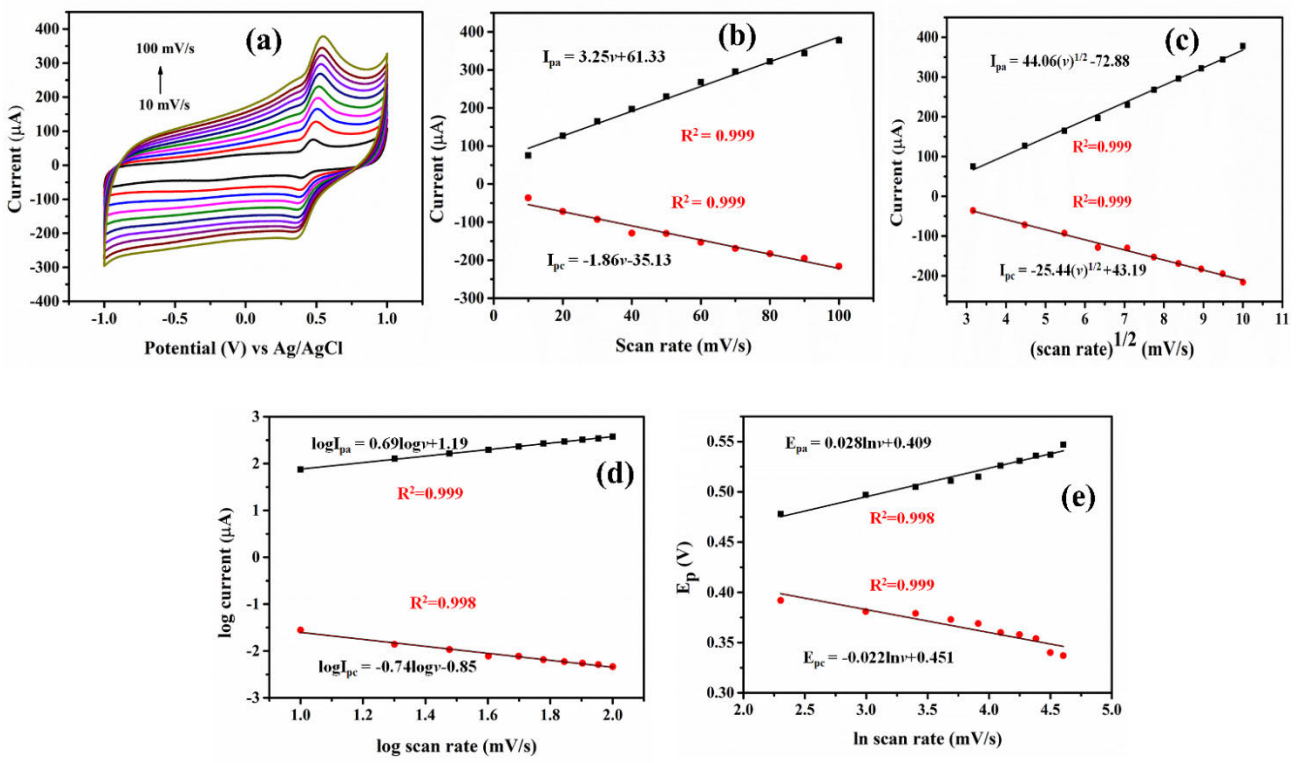

FIGURE 7. (a) The effect of scan rate of N-richSRGO modified electrode was studied in PBS pH = 3 with 1 mM DA at different scan rates (10–100 mV/s), (b) I_p vs. (v), (c)I_p vs $v^{1/2}$, (d) Log I_p vs Log$v$ and (e) E_p vs. ln v.

TABLE 1. Comparison of the current work with the other published work on different modified electrodes for DA sensing.

ELECTRODE	SENSITIVITY	LINEAR RANGE	LOD μM	LOQ* μM	REF
[a]*PoPD/E-RGO modified electrode*	-	*10-400 μM and 400-800μM*	*7.5*	*25*	[50]
[b]*{Nf-fc}-MME modifed electrode*	*1.1 μA/mM*	*250μM-5 mM*	*22.7*	*75.6*	[51]
[c]*Ferrocene/Pd-linked modifed electrode*	*0.125μA/mM*	-	*50*	*166.6*	[52]
[d]*CuO-MgO modifed electrode*	*69 μA/mM cm^2*	*10-100μM*	*6.4*	*21.3*	[53]
N-rich SRGO-modified electrode	***142 μA/mM***	***150-350μM***	***9.3***	***31***	***This work***

[a]*poly(o-phenylenediamine) functionalized with electrochemically reduced graphene oxide,*
[b] *ferrocene bound Nafion membrane modified electrode,*
[c] *ferrocene encapsulated palladium-linked ormosil,*
[d]*copper oxide-magnesium oxide,*
**LOQ values for other papers were calculated using equation (7).*

attributed to enhanced electrical conductivity, stable dispersion, and favorable biocompatibility associated with the N-rich SRGO modification.

4) REPRODUCIBILITY AND SELECTIVITY

The reproducibility of the developed DA sensor was investigated using five electrodes that were prepared using similar protocols. Fig.9a demonstrates the DA sensing using 0.1 M PBS at pH 3. The negligible difference in the current value within the five modified electrodes concludes that the developed dopamine sensor is highly reproducible. It is widely acknowledged that AA and UA with higher concentrations coexist with DA in human body fluids. Therefore, we have studied the DA sensing of N-rich SRGO in the presence of other interfering species, such as NaCl, KCl, glucose, sucrose, AA, and UA (Fig. 9b), using an amperometric technique at 0.5 V. The negligible increase in the current values indicates that the N-rich SRGO-modified electrode is highly selective towards DA, even at higher concentrations of other interferents.

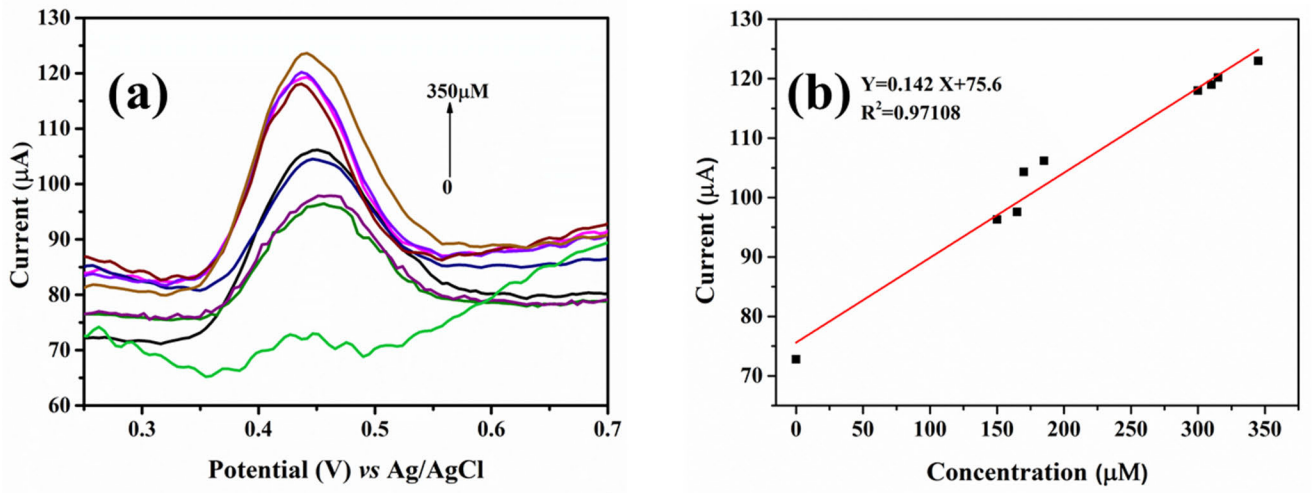

FIGURE 8. (a) Differential pulse voltammetry studies of the N-rich SRGO-modified electrode towards a successive increase in DA concentration, (b) the calibration plot between peak current *vs.* DA concentration.

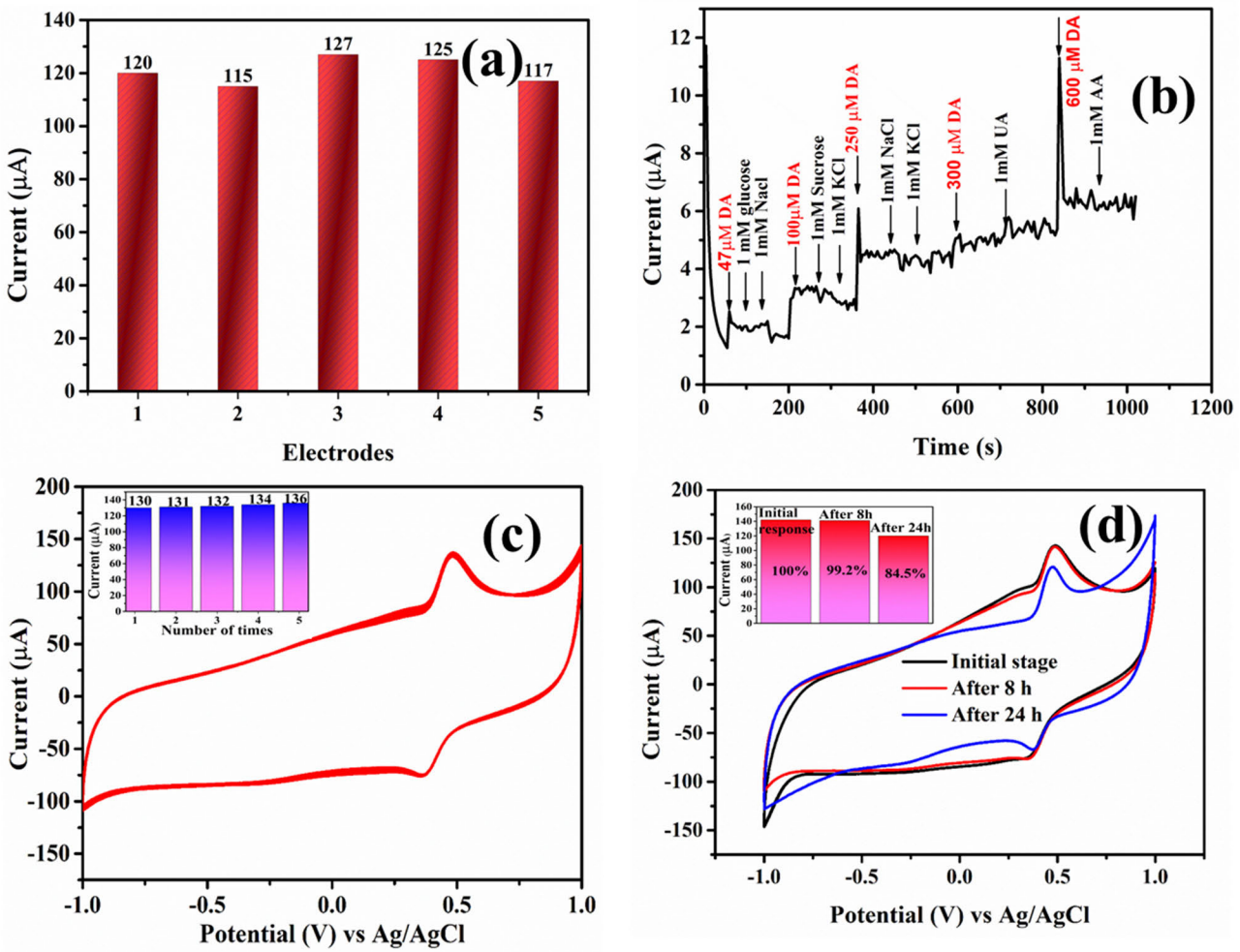

FIGURE 9. (a) Reproducibility studies of five different N-rich SRGO-modified electrodes for the detection of 1 mM DA, (b) Interference analysis,(c) Repeatability and (d) Reusability of N-rich SRGO modified electrode in the presence of 1 mM DA (PBS pH 3).

5) REPEATABILITY AND REUSABILITY

The relative standard deviation (RSD) of about 1.82 % for five repeated voltammetric measurements (Fig. 9c) on the same electrode demonstrated the DA sensor has excellent repeatability. In addition, the reusability of the DA sensor was investigated over different periods. The retention of 84.5%

initial current at the same oxidation potential (Fig.9d) after 24 h confirmed the reusability of the N-rich SRGO-modified electrode for DA sensing.

IV. CONCLUSION

This study employed a straightforward, cost-effective hydrothermal method to synthesize a novel N-rich SRGO material. The incorporation of nitrogen and sulfur, possessing higher electronegativity, onto the graphene structure not only provided abundant electroactive sites but also yielded a superior oxidation current of 345 μA compared to RGO, NRGO, and NSRGO in the presence of standard ferro/ferric redox. The developed N-rich SRGO-modified electrode, featuring an enhanced electron transfer rate, was successfully applied to detect DA. The proposed N-rich SRGO-modified electrode demonstrated a sensitivity of 142 μA/mM and a detection limit of 9.3 μM over a broad linear range of 150-350 μM, surpassing the performance of metal/metal oxide and polymer-based modified electrodes. The N-rich SRGO-modified electrode also demonstrated excellent repeatability, stability, and high selectivity in detecting DA amidst interfering substances such as AA, UA, glucose, and sucrose.

REFERENCES

[1] D. W. Kimmel, G. LeBlanc, M. E. Meschievitz, and D. E. Cliffel, "Electrochemical sensors and biosensors," *Anal. Chem.*, vol. 84, no. 2, pp. 685–707, Jan. 2012.

[2] K. Beaver, A. Dantanarayana, and S. D. Minteer, "Materials approaches for improving electrochemical sensor performance," *J. Phys. Chem. B*, vol. 125, no. 43, pp. 11820–11834, Nov. 2021.

[3] R. Chen, N. Nioradze, P. Santhosh, Z. Li, S. P. Surwade, G. J. Shenoy, D. G. Parobek, M. A. Kim, H. Liu, and S. Amemiya, "Ultrafast electron transfer kinetics of graphene grown by chemical vapor deposition," *Angew. Chem.*, vol. 127, no. 50, pp. 15349–15352, Dec. 2015.

[4] Y. Zhu, S. Murali, W. Cai, X. Li, J. W. Suk, J. R. Potts, and R. S. Ruoff, "Graphene and graphene oxide: Synthesis, properties, and applications," *Adv. Mater.*, vol. 22, pp. 3906–3924, Sep. 2010.

[5] A. K. Geim and K. S. Novoselov, "The rise of graphene," *Nature Mater.*, vol. 6, no. 3, pp. 183–191, Mar. 2007.

[6] J. G. S. Moo, A. Ambrosi, A. Bonanni, and M. Pumera, "Inherent electrochemistry and activation of chemically modified graphenes for electrochemical applications," *Chem. Asian J.*, vol. 7, no. 4, pp. 759–770, Apr. 2012.

[7] M. Pumera, "Electrochemistry of graphene: New horizons for sensing and energy storage," *Chem. Rec.*, vol. 9, no. 4, pp. 211–223, Sep. 2009.

[8] T. A. S. L. de Sousa, V. C. F. dos Santos, N. B. F. Almeida, F. A. dos Santos, T. G. da Silva, E. N. D. de Araujo, A. S. R. de Andrade, and F. Plentz, "Surface modifications in graphene by DNA aptamers for *Staphylococcus aureus* detection," *IEEE Sensors J.*, vol. 21, no. 23, pp. 26534–26541, Dec. 2021.

[9] B. Chakraborty and C. Roychaudhuri, "Metal/metal oxide modified graphene nanostructures for electrical biosensing applications: A review," *IEEE Sensors J.*, vol. 21, no. 16, pp. 17629–17642, Aug. 2021.

[10] X. Dong, Y. Ma, G. Zhu, Y. Huang, J. Wang, M. B. Chan-Park, L. Wang, W. Huang, and P. Chen, "Synthesis of graphene-carbon nanotube hybrid foam and its use as a novel three-dimensional electrode for electrochemical sensing," *J. Mater. Chem.*, vol. 22, no. 33, pp. 17044–17048, 2012.

[11] S. Woo, Y.-R. Kim, T. D. Chung, Y. Piao, and H. Kim, "Synthesis of a graphene–carbon nanotube composite and its electrochemical sensing of hydrogen peroxide," *Electrochimica Acta*, vol. 59, pp. 509–514, Jan. 2012.

[12] L. Chandrasekar and K. P. Pradhan, "Self-consistent modeling of B or N substitution doped bottom gated graphene FET with nonzero bandgap," *IEEE Trans. Electron Devices*, vol. 68, no. 7, pp. 3658–3664, Jul. 2021.

[13] M. Saleh-Mohammadnia, M. Ghalkhani, H. Roghani-Mamaqani, S. Hemmati, and H. Mardani, "Amine-grafted graphene oxide functionalized with N,S-doped carbon dots: Sensitive electrochemical sensor for metronidazole determination," *IEEE Sensors J.*, vol. 23, no. 17, pp. 18986–18993, 2023.

[14] M. Yuan, F. Luo, Y. Rao, W. Ying, J. Yu, H. Li, and X. Chen, "Laser in situ preparation of S-doped porous graphene for flexible microsupercapacitors," *IEEE Electron Device Lett.*, vol. 43, no. 2, pp. 327–330, Feb. 2022.

[15] Y. Cao, W. Si, Y. Zhang, Q. Hao, W. Lei, X. Xia, J. Li, and F. Wang, "Nitrogen-doped graphene: Effect of graphitic-N on the electrochemical sensing properties towards acetaminophen," *FlatChem*, vol. 9, pp. 1–7, May 2018.

[16] C. T. Fakude, O. A. Arotiba, R. Moutloali, and N. Mabuba, "Nitrogen-doped graphene electrochemical sensor for selenium (IV) in water," *Int. J. Electrochem. Sci.*, vol. 14, no. 10, pp. 9391–9403, Oct. 2019.

[17] X. Li, H. Zhao, L. Shi, X. Zhu, M. Lan, Q. Zhang, and Z. Hugh Fan, "Electrochemical sensing of nicotine using screen-printed carbon electrodes modified with nitrogen-doped graphene sheets," *J. Electroanal. Chem.*, vol. 784, pp. 77–84, Jan. 2017.

[18] Z.-H. Sheng, X.-Q. Zheng, J.-Y. Xu, W.-J. Bao, F.-B. Wang, and X.-H. Xia, "Electrochemical sensor based on nitrogen doped graphene: Simultaneous determination of ascorbic acid, dopamine and uric acid," *Biosensors Bioelectron.*, vol. 34, no. 1, pp. 125–131, Apr. 2012.

[19] M. Li, C. Liu, H. Zhao, H. An, H. Cao, Y. Zhang, and Z. Fan, "Tuning sulfur doping in graphene for highly sensitive dopamine biosensors," *Carbon*, vol. 86, pp. 197–206, May 2015.

[20] S. R. Kanuganti, R. Sultana, D. Kolli, G. K. Maddula, and M. R. Singampalli, "Facile one pot synthesis of sulphur doped graphene for non-enzymatic sensing of hydrogen peroxide," *Int. J. Environ. Anal. Chem.*, vol. 103, no. 19, pp. 8051–8062, Dec. 2023.

[21] L. Magerusan, F. Pogacean, S. Rada, and S. Pruneanu, "Sulphur-doped graphene based sensor for rapid and efficient gallic acid detection from food related samples," *J. Taiwan Inst. Chem. Engineers*, vol. 140, Nov. 2022, Art. no. 104539.

[22] W. Lei, W. Si, Q. Hao, Z. Han, Y. Zhang, and M. Xia, "Nitrogen-doped graphene modified electrode for nimodipine sensing," *Sens. Actuators B, Chem.*, vol. 212, pp. 207–213, Jun. 2015.

[23] K. P. Prathish, M. M. Barsan, D. Geng, X. Sun, and C. M. A. Brett, "Chemically modified graphene and nitrogen-doped graphene: Electrochemical characterisation and sensing applications," *Electrochimica Acta*, vol. 114, pp. 533–542, Dec. 2013.

[24] R. Zhang, C. Zhang, F. Zheng, X. Li, C.-L. Sun, and W. Chen, "Nitrogen and sulfur co-doped graphene nanoribbons: A novel metal-free catalyst for high performance electrochemical detection of 2, 4, 6-trinitrotoluene (TNT)," *Carbon*, vol. 126, pp. 328–337, Jan. 2018.

[25] Y. Tian, Y. Ma, H. Liu, X. Zhang, and W. Peng, "One-step and rapid synthesis of nitrogen and sulfur co-doped graphene for hydrogen peroxide and glucose sensing," *J. Electroanal. Chem.*, vol. 742, pp. 8–14, Apr. 2015.

[26] G. Chen, Y. Liu, Y. Liu, Y. Tian, and X. Zhang, "Nitrogen and sulfur dual-doped graphene for glucose biosensor application," *J. Electroanal. Chem.*, vol. 738, pp. 100–107, Feb. 2015.

[27] P. Guo, F. Xiao, Q. Liu, H. Liu, Y. Guo, J. R. Gong, S. Wang, and Y. Liu, "One-pot microbial method to synthesize dual-doped graphene and its use as high-performance electrocatalyst," *Sci. Rep.*, vol. 3, no. 1, p. 3499, Dec. 2013.

[28] L. Xiao, J. Yin, Y. Li, Q. Yuan, H. Shen, G. Hu, and W. Gan, "Facile one-pot synthesis and application of nitrogen and sulfur-doped activated graphene in simultaneous electrochemical determination of hydroquinone and catechol," *Analyst*, vol. 141, no. 19, pp. 5555–5562, 2016.

[29] J. Han, Y. Zhang, Z. Chen, A. Zhang, and X. Shi, "Synergistic effect of nitrogen and sulfur co-doped holey graphene for sensitive fenitrothion detection supported by DFT study," *Microchemical J.*, vol. 193, Oct. 2023, Art. no. 109218.

[30] M. Megawati, C. K. Chua, Z. Sofer, K. Klímová, and M. Pumera, "Nitrogen-doped graphene: Effect of graphite oxide precursors and nitrogen content on the electrochemical sensing properties," *Phys. Chem. Chem. Phys.*, vol. 19, no. 24, pp. 15914–15923, 2017.

[31] M. O. Klein, D. S. Battagello, A. R. Cardoso, D. N. Hauser, J. C. Bittencourt, and R. G. Correa, "Dopamine: Functions, signaling, and association with neurological diseases," *Cellular Mol. Neurobiol.*, vol. 39, no. 1, pp. 31–59, Jan. 2019.

[32] N. Agrawal, B. Zhang, C. Saha, C. Kumar, B. K. Kaushik, and S. Kumar, "Development of dopamine sensor using silver nanoparticles and PEG-functionalized tapered optical fiber structure," *IEEE Trans. Biomed. Eng.*, vol. 67, no. 6, pp. 1542–1547, Jun. 2020.
[33] H. Landari, Y. Messaddeq, and A. Miled, "Microscope-FTIR spectrometry based sensor for neurotransmitters detection," *IEEE Trans. Biomed. Circuits Syst.*, vol. 15, no. 5, pp. 938–948, Oct. 2021.
[34] D. Zhang, M. Qian, X. Yang, C. Zhang, H. Qi, and H. Qi, "Label-free electrogenerated chemiluminescence aptasensing method for highly sensitive determination of dopamine via target-induced DNA conformational change," *Anal. Chem.*, vol. 95, no. 13, pp. 5500–5506, Apr. 2023.
[35] X. Liu, Y. Fang, D. Zhu, J. Wang, Y. Wu, T. Wang, and Y. Wang, "Hollow structure molecularly imprinted ratiometric fluorescence sensor for the selective and sensitive detection of dopamine," *Analyst*, vol. 148, no. 12, pp. 2844–2854, 2023.
[36] F. B. K. Eddin, Y. W. Fen, J. Y. C. Liew, N. I. M. Fauzi, W. M. E. M. M. Daniyal, and H. Abdullah, "Development of plasmonic-based sensor for highly sensitive and selective detection of dopamine," *Opt. Laser Technol.*, vol. 161, Jun. 2023, Art. no. 109221.
[37] M. Roushani and Z. M. Karazan, "Novel electrochemical sensor based on electropolymerized dopamine molecularly imprinted polymer for selective detection of pantoprazole," *IEEE Sensors J.*, vol. 22, no. 7, pp. 6263–6269, Apr. 2022.
[38] J. Yang, J. Yan, R. Chen, and H. Ni, "Photo-refreshable electrochemical sensor based on composite electrode of carbon nanotubes and TiO_2 nanoparticles," *IEEE Sensors J.*, vol. 19, no. 9, pp. 3212–3216, May 2019.
[39] S. Rong, P. Zhang, L. Zou, Y. Tian, M. Miao, D. Jia, R. Qiu, F. Qi, H. Ma, and H. Pan, "Electrochemical determination of dopamine at Nafion and β-cyclodextrin-functionalized multi-walled carbon nanotubes composite modified glassy carbon electrode," *IEEE Sensors J.*, vol. 22, no. 6, pp. 5540–5547, 2022.
[40] R. Muralidharan, V. Chandrashekhar, D. Butler, and A. Ebrahimi, "A smartphone-interfaced, flexible electrochemical biosensor based on graphene ink for selective detection of dopamine," *IEEE Sensors J.*, vol. 20, no. 22, pp. 13204–13211, Nov. 2020.
[41] R. D'Orsi, V. C. Canale, R. Cancelliere, O. H. Omar, C. Mazzuca, L. Micheli, and A. Operamolla, "Tailoring the chemical structure of cellulose nanocrystals by amine functionalization," *Eur. J. Organic Chem.*, vol. 26, no. 11, Mar. 2023, Art. no. e202201457.
[42] D. C. Marcano, D. V. Kosynkin, J. M. Berlin, A. Sinitskii, Z. Sun, A. Slesarev, L. B. Alemany, W. Lu, and J. M. Tour, "Improved synthesis of graphene oxide," *ACS Nano*, vol. 4, no. 8, pp. 4806–4814, Aug. 2010.
[43] T. Wang, L.-X. Wang, D.-L. Wu, W. Xia, and D.-Z. Jia, "Interaction between nitrogen and sulfur in co-doped graphene and synergetic effect in supercapacitor," *Sci. Rep.*, vol. 5, no. 1, p. 9591, Apr. 2015.
[44] J. Lavanya and N. Gomathi, "High-sensitivity ascorbic acid sensor using graphene sheet/graphene nanoribbon hybrid material as an enhanced electrochemical sensing platform," *Talanta*, vol. 144, pp. 655–661, Nov. 2015.
[45] G. Hu, Y. Ma, Y. Guo, and S. Shao, "Electrocatalytic oxidation and simultaneous determination of uric acid and ascorbic acid on the gold nanoparticles-modified glassy carbon electrode," *Electrochimica Acta*, vol. 53, no. 22, pp. 6610–6615, Sep. 2008.
[46] G. Leftheriotis, S. Papaefthimiou, and P. Yianoulis, "Dependence of the estimated diffusion coefficient of Li_xWO_3 films on the scan rate of cyclic voltammetry experiments," *Solid State Ionics*, vol. 178, nos. 3–4, pp. 259–263, Feb. 2007.
[47] E. Laviron, "General expression of the linear potential sweep voltammogram in the case of diffusionless electrochemical systems," *J. Electroanal. Chem.*, vol. 101, no. 1, pp. 19–28, Jul. 1979.
[48] W. Song, Y. Chen, J. Xu, and D. B. Tian, "A selective voltammetric detection for dopamine using poly (gallic acid) film modified electrode," *Chin. Chem. Lett.*, vol. 21, no. 3, pp. 349–352, Mar. 2010.
[49] F. Lopes, J. G. Pacheco, P. Rebelo, and C. Delerue-Matos, "Molecularly imprinted electrochemical sensor prepared on a screen printed carbon electrode for naloxone detection," *Sens. Actuators B, Chem.*, vol. 243, pp. 745–752, May 2017.
[50] X. Liu, H. Zhu, and X. Yang, "An electrochemical sensor for dopamine based on poly(o-phenylenediamine) functionalized with electrochemically reduced graphene oxide," *RSC Adv.*, vol. 4, no. 8, pp. 3743–3749, 2014.
[51] A. S. Kumar, P. Swetha, and K. C. Pillai, "Enzyme-less and selective electrochemical sensing of catechol and dopamine using ferrocene bound Nafion membrane modified electrode," *Anal. Methods*, vol. 2, no. 12, pp. 1962–1968, 2010.
[52] P. C. Pandey, S. Upadhyay, I. Tiwari, G. Singh, and V. S. Tripathi, "A novel ferrocene encapsulated palladium-linked ormosil-based electrocatalytic dopamine biosensor," *Sens. Actuators B, Chem.*, vol. 75, nos. 1–2, pp. 48–55, Apr. 2001.
[53] S. Paramparambath, S. Shafath, M. R. Maurya, J.-J. Cabibihan, A. Al-Ali, R. A. Malik, and K. K. Sadasivuni, "Nonenzymatic electrochemical sensor based on CuO-MgO composite for dopamine detection," *IEEE Sensors J.*, vol. 21, no. 22, pp. 25597–25605, Nov. 2021.

J. LAVANYA received the B.Sc. degree in physics from Periyar University, Tamilnadu, India, the M.Sc. degree in physics from Annamalai University, Tamilnadu, the M.Tech. degree in nanotechnology from Karunya University, Tamilnadu, and the Ph.D. degree from the Department of Chemistry, Indian Institute of Space Science and Technology, India. Currently, she is a Postdoctoral Fellow with the Center for Innovation and Product Development, Vellore Institute of Technology, Chennai, India. Her research interests include nanomaterials and electrochemical sensors.

M. AAKASH received the B.Sc. and M.Sc. degrees in physics from the University of Madras. He is currently pursuing the Ph.D. degree with the School of Advanced Sciences, Center for Innovation and Product Development, Vellore Institute of Technology, Chennai, India. His research interests include nanomaterials and electrochemical sensors.

A. RAVI SANKAR (Senior Member, IEEE) received the B.E. degree from the University of Madras, the M.E. degree from the PSG College of Technology (Bharathiar University), and the Ph.D. degree from Indian Institute of Technology Kharagpur (IITKgp), Kharagpur. From February 2008 to June 2009, he was a Project Scholar with the Advanced Technology Development Centre, IIT, Kharagpur, where he was involved in designing, fabricating, and testing MEMS sensors. From 2009 to 2011, he was an Associate Professor with the Department of Electronics and Communications Engineering, Karunya University, Coimbatore. Since June 2011, he has been a Professor with the School of Electronics Engineering (SENSE), Vellore Institute of Technology (VIT), Chennai Campus. He has had a joint affiliation with the Centre for Innovation and Product Development (CIPD), VIT Chennai, since 2020. His research interests include VLSI design, MEMS and microsystems, nanomaterials, and nanosensors development.

N. GOMATHI received the B.Tech. degree in chemical engineering from the University of Madras, Chennai, India, the M.Tech. degree in chemical engineering from Bharathiyar University, Coimbatore, India, and the Ph.D. degree from Indian Institute of Technology Kharagpur, India. She joined as an Assistant Professor with the Department of Chemistry, Indian Institute of Space Science and Technology, Trivandrum, Kerala, India, where she is currently a Professor. Her research interests include plasma surface modification, surface functionalization of polymers, enhancement of bio and blood compatibility, biosensors, nanocomposite, and metal-organic frameworks.